Chinese Chemical Letters 35 (2024) 109458

Contents lists available at ScienceDirect

Chinese Chemical Letters

journal homepage: www.elsevier.com/locate/cclet

Unprecedented sesquiterpene-polycyclic polyprenylated acylphloroglucinol adduct against acute myeloid leukemia *via* inhibiting mitochondrial complex V

Zhengyi Shi[1], Jie Yin[1], Yang Xiao, Zhangrong Hou, Fei Song, Jianping Wang, Qingyi Tong*, Changxing Qi*, Yonghui Zhang*

Hubei Key Laboratory of Natural Medicinal Chemistry and Resource Evaluation, School of Pharmacy, Tongji Medical College, Huazhong University of Science and Technology, Wuhan 430030, China

ARTICLE INFO

Article history:
Received 31 October 2023
Revised 22 December 2023
Accepted 22 December 2023
Available online 29 December 2023

Keywords:
PPAP adduct
Single-crystal X-ray diffraction
Keto-enol tautomerism
Plausible biosynthetic pathway
Cytotoxic activity

ABSTRACT

Monosescinol A (**1**), the first example of sesquiterpene–polycyclic polyprenylated acylphloroglucinol (PPAP) adduct, which represented a new subclass of PPAP-type natural products, along with two new congeners with normal spiro 6/6/5 tricyclic architecture, were isolated from *Hypericum longistylum*. Monosescinol A possessed an unprecedented 6/5/5/6/6 pentacyclic carbon skeleton that might be assembled from the 6/6/5 carbon skeleton, *via* the splitting decomposition of C-3/C-14, and the attack from the C-3 in the PPAP core to C-28 in sesquiterpene section. In addition, we have firstly confirmed that 24*R* configuration was existed in *sec*–Bu containing PPAPs by single crystal diffraction data analysis of monosescinol B (**2**), that might provide an enlightenment in the configurational determination of *sec*–Bu containing PPAPs. Significantly, further pharmacological research has found that compound **1** exhibited remarkable pharmacological effects against acute myeloid leukemia (AML) cell lines, with direct inhibition of mitochondrial complex V and an increase in mitochondrial membrane potential, and led to an induction of oxidative stress, endogenous inflammation, and apoptosis of AML cells.

Acute myeloid leukemia (AML) is one of the most common hematological malignancies in adults, accounting for approximately 33% of all leukemias worldwide. The annual incidence of AML in the US and China is over 20,000 and 30,000 cases, respectively, resulting in serious implications for the population health worldwide. Despite many advances, AML still carries a poor prognosis, and around only 25% of the patients survive longer than five years after the diagnosis. Thus, it is still a significant healthy problem for human to continue the scientific research for potential and effective drugs to against AML [1,2].

Polycyclic polyprenylated acylphloroglucinols (PPAPs) are a broad family of natural products decorated from the highly oxygenated acylphloroglucinol-derived cores and featured by the subsistence of isoprenyl or geranyl groups [3]. In consideration of their intriguing chemical structures, PPAPs have been reported to show diverse activities [3,4]. In our continuous efforts for the discovery of active natural products, a sesquiterpene-PPAP adduct with unprecedented carbon skeleton, monosescinol A (**1**), and two new congeners, monosescinols B (**2**), which was firstly determined by the single crystal that C-24 was *R*, and C (**3**) with normal 6/6/5 tricyclic skeleton (Fig. 1), were isolated from *Hypericum longistylum*. Significantly, compound **1** was the first example of natural products generating by the fusion of PPAP with sesquiterpene segment to form the unparalleled sesquiterpene–PPAP adduct, that represented a new category of PPAP derivatives. The splitting decomposition of C-3/C-14 in the normal 6/6/5 skeleton and the attack from C-3 in the acylphloroglucinol core of the PPAP moiety to C-28 in the sesquiterpene fragment has been proposed to be the key step in the biosynthetic pathway of **1**. More prominently, compound **1** displayed outstanding anticancer activity against AML cell lines by inhibiting mitochondrial complex V and increasing mitochondrial membrane potential, and causing oxidative stress, endogenous inflammation and apoptosis of AML cell. Herein, we report the details for the isolation, structural elucidation, and biological evaluation of **1**–**4**, as well as their plausible biogenetic pathway [6–14].

Monosescinol A (**1**), finally acquired as needle crystal, was identified as $C_{42}H_{64}O_6$ based on its high resolution electrospray ionization mass spectroscopy (HRESIMS) data (*m/z*: $[M+Na]^+$, calcd. 687.4601; found 687.4608), which indicated eleven indices

* Corresponding authors.
E-mail addresses: qytong@hust.edu.cn (Q. Tong), qichangxing@hust.edu.cn (C. Qi), zhangyh@mails.tjmu.edu.cn (Y. Zhang).
[1] These authors contributed equally to this work.

https://doi.org/10.1016/j.cclet.2023.109458
1001-8417/

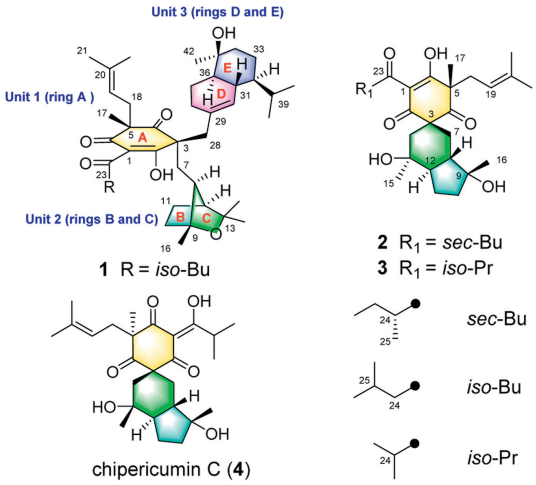

Fig. 1. The structures of compounds **1**–**4**.

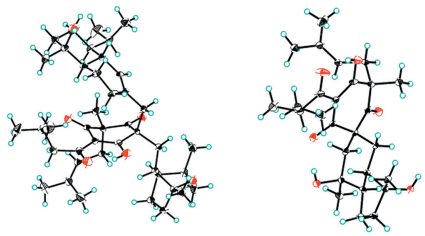

Fig. 2. X-ray structures of **1** (left) and **2** (right).

of hydrogen deficiency. The ^{13}C NMR and DEPT spectra exhibited 42 signals including eleven methyl, ten methylene, and nine methine (two olefinic) groups, as well as twelve nonprotonated carbon atoms (two olefinic and three carbonyl). The above evidence indicated that **1** was a PPAP-type metabolite featuring a pentacyclic ring system [3–5,9–13].

The planar structure of **1** could be fully identified *via* the interpretation of its 2D NMR spectrum analysis. The heteronuclear multiple bond correlation (HMBC) from H_3-17 to C-4, C-5, C-6 and C-18; from H_2-7/H_2-28 to C-2, C-3, and C-4; from H-25 to C-23; from H_3-21 to C-19, C-20 and C-22, and the ^1H–^1H correlation spectroscopy (COSY) cross-peaks of H_2-24/H-25/H_3-26/H_3-27, and of H_2-18/H-19, coupled with the comparison of chemical shifts of the congeners with similar fragment, sufficiently confirmed ring A was the acylphloroglucinol core (unit 1) [8–13]. Additionally, the HMBC correlations from H_3-14 to C-12, C-13 and C-15, and from H_3-16 to C-8, C-9 and C-10, as well as the ^1H–^1H COSY cross-peaks of H-8/H-12/H_2-11/H_2-10 and the chemical shifts of C-9 (δ_C 85.9) and C-13 (δ_C 79.2), which determined that there was an oxygen bridge between them, established the connection type of unit 2. Furthermore, the HMBC correlations from H_2-28 to C-29, C-30 and C-38, H_3-42 to C-34, C-35 and C-36, and H_3-40 to C-32, as well as the ^1H–^1H COSY cross-peaks of H-30/H-31/H-32/H_2-33/H_2-34/H-36/H_2-37/H-38 and H_3-40/H-39/H_3-41 safely construct the attended mode of the sesquiterpene moiety (unit 3). Eventually, the key HMBC correlations from H_2-7 to C-2, C-3 and C-4 and ^1H–^1H COSY cross-peak of H_2-7/H-8 revealed that the unit 2 was connected to unit 1 *via* the C-3–C-7–C-8 linkage, and the pivotal HMBC correlations from H_2-28 to C-2, C-3, C-4, C-29, C-30 and C-38 expounded the unit 3 was attached at unit 1 by the C-3–C-28–C-29 bond. Thus, the planar structure of **1** was defined.

In its nuclear Overhauser effect spectroscopy (NOESY) spectrum, the correlations of H-8/H-12/H-11a/H_3-16 could assign the orientation of these groups in the unit 2. In addition, the NOESY correlations of H-31/H-33a/H_3-40/H-37b indicated that the isopropyl group, H-33a, H-37b and H-31 in the unit 3 were homolateral, and the correlations of H-36/H-37a/H_3-42 indicated that those groups, as well as H-32, were located in the same side. Moreover, the clear NOESY correlations of H-18a/H-8, H-18a/H-12 and H-18b/H-12 indicated that the isopentenyl group (C-18–C-19–C-20–C-21–C-22) at C-5 in unit 1 was located at the identical side with the unit 2 and the obvious NOESY correlations of H_3-17/H-30 and H_3-17/H-39 also identified that CH_3-17 and sesquiterpene moiety were on the same side. However, the relative configurations between the units 1, 2 and 3 in **1** were unclear due to the structural independent ability of those three units. Therefore, we have tried to identify the relative configuration of **1** by single-crystal X-ray diffraction experiments. After repeated efforts with different conditions, a suitable crystal was finally obtained in the acetonitrile–acetone–water (6:3:1) system. Based on the Flack parameter of 0.09(4) (CCDC No. 2225541), the relative and absolute configurations of **1** could be straightforwardly stated (Fig. 2). Conclusively, by the systematic analysis above, we could unquestionably appoint the structure of this isolate **1** with the unparalleled 6/5/5/6/6 pentacyclic ring system and the C-2 position was an enol structure.

The structure of monosescinol B (**2**) with common 6/6/5 skeleton was built by its nuclear magnetic resonance (NMR) data and finally confirmed by the single crystal diffraction tests. Actually, we have initially identified the configuration of C-24 was "*S*" in **2** based on the "24*S* rule" that had been widely applied to identify the configuration of C-24 of *sec*–Bu containing PPAPs [14]. Due to almost all reported *sec*–Bu containing PPAPs possessing the 24*S* configuration in the *sec*–Bu moiety, the previously studies considered that the C-24 should be "*S*" for the biosynthesis consideration for a long time. In our research, the single crystal diffraction

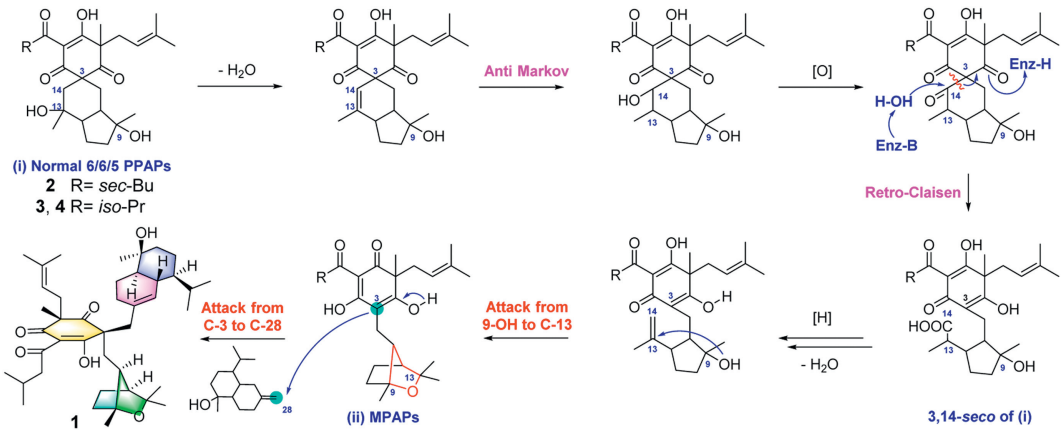

Scheme 1. The plausible biosynthetic pathway of compounds **1**–**4**.

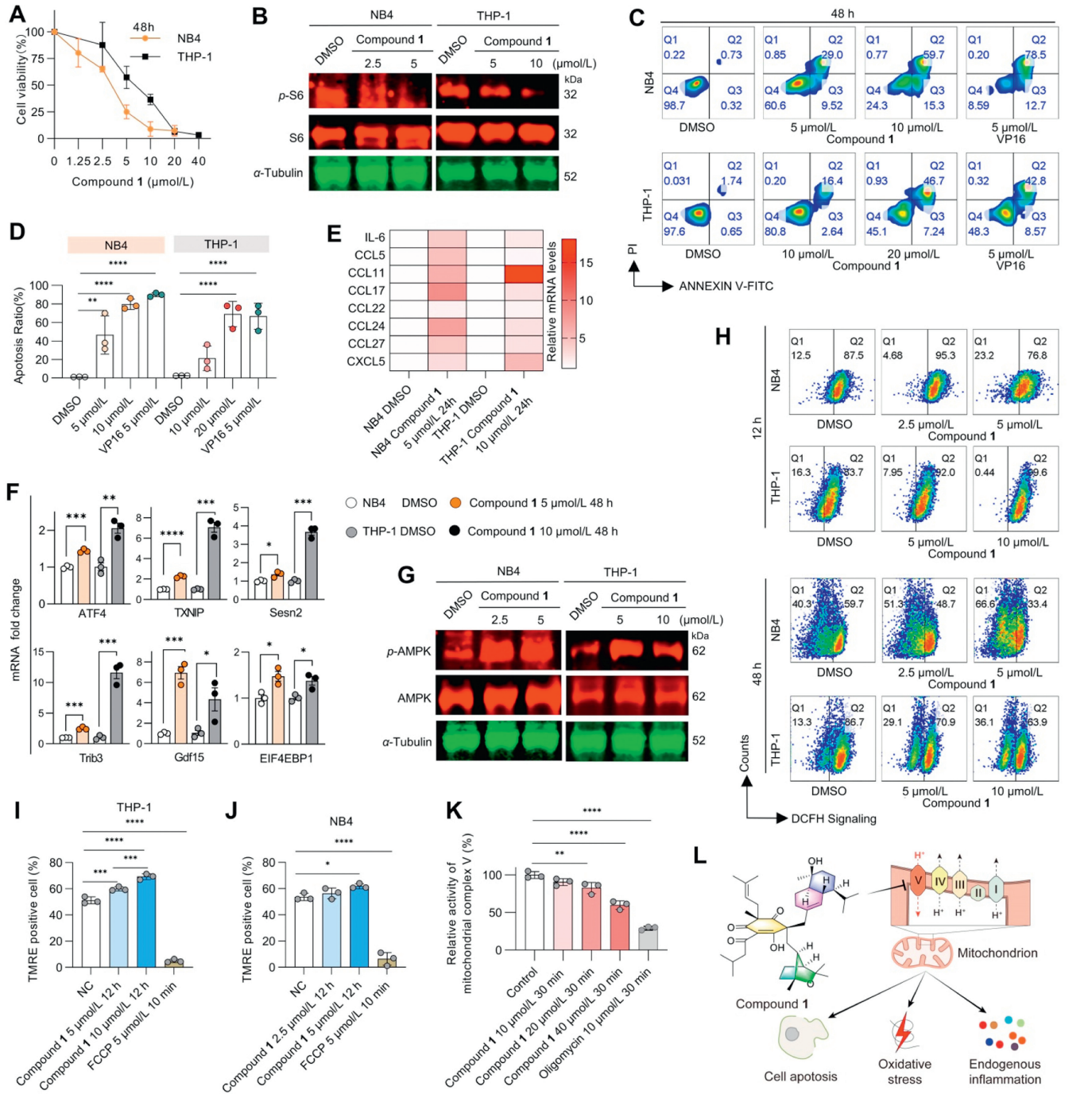

Fig. 3. Compound **1** is a new skeleton compound targeting mitochondrial complex V. (A) Cell viability curve of NB4 and THP-1 cells after exposure to increasing doses of compound **1** for 48 h. $n = 3$. (B) Western blot analysis of total and phosphorylated forms of ribosomal protein S6, α-tubulin was used as an internal reference, the same as below. (C, D) The apoptosis ratio of cells was measured by flow cytometry. $n = 3$. DMSO (<0.1%) and VP16 were used as controls. (E) mRNA expression of cytokines or chemokines analyzed by qPCR. (F) mRNA expression of oxidative stress-related genes analyzed by qPCR. $n = 3$. (G) Western blot analysis of AMPK and phospho-AMPK (p-AMPK). (H) Cellular ROS content in AML cells was analyzed by flow cytometry. $n = 3$. (I, J) The mitochondrial membrane potential in AML cells was analyzed by flow cytometry. $n = 3$. (K) Mitochondrial complex V activity analysis. $n = 3$. (L) Diagram of the pharmacological mechanism of compound **1**. Mean±standard deviation (SD), two-way ANOVA. $^{*}P < 0.05$, $^{**}P < 0.01$, $^{***}P < 0.005$, $^{****}P < 0.001$.

test of **2** was performed. Surprising, the high-quality single crystal diffraction data [Flack parameter 0.01(18); CCDC No. 2303265] undisputedly confirmed the 24*R* configuration of **2** and uncovered that the "24*S* rule" was unreliable. Thus, our discovery revealed that the configurational determination of C-24 in the *sec*–Bu containing PPAPs should be more cautious, and this might be confirmed only get through single crystal diffraction tests but not by the biosynthesis and stoichiometric calculation. The structure of monosescinol C (**3**) was similar with **2**, with the only difference was a *sec*–butyl at C-23 in **2** but isopropyl in **3**. The detailed structural analysis of **2** and **3** were provided in Supporting information.

Structurally, compound **1** was the first example of sesquiterpene–PPAP adduct, which represented a new subclass of PPAP-type natural products. Therefore, the plausible biosynthetic pathway to **1** was proposed. The PPAP fragment (units 1 and 2) was originated from the acylphloroglucinol core *via* the methylation, prenylation and geranylation, the cleavage between C-3 and C-14, as well as the cyclization reactions between 9-OH and C-13. Subsequently,

the attack from C-3 in the acylphloroglucinol core to C-28 in the sesquiterpene unit was finally generated this first sesquiterpene fused PPAP (Scheme 1) [6–14].

Compound **1** showed significant anticancer activity against a variety of cancer cell lines, especially AML. The half maximal inhibitory concentration (IC_{50}) values of compound **1** for NB4 and THP-1 cells were 3.588 μmol/L and 5.760 μmol/L, respectively (Fig. 3A and Table S1 in Supporting information). In sharp contrast, compound **1** has an IC_{50} of 56.979 μmol/L in the normal cell line NCM460, implying that compound **1** has specific antitumor effects rather than general cytotoxicity. Further experiments revealed that the growth inhibitory effect of compound **1** may stem from an inhibitory effect on protein synthesis in AML cells, as we observed significant downregulation of phosphorylation levels of ribosomal protein S6 (Fig. 3B). Furthermore, after 48 h of treatment with compound **1**, obvious apoptosis was observed in AML cells, and the proportion of apoptosis exceeded 60% in the high-dose treatment group (Figs. 3C and D). In addition, we found that in AML cells, compound **1** significantly upregulated the mRNA levels of cytokines or chemokines and promoted endogenous inflammation (Fig. 3E).

To further explore the cytotoxic mechanism of compound **1**, we investigated the effects of this compound on oxidative stress-related genes and adenosine 5′-monophosphate-activated protein kinase (AMPK) a key kinase in the regulation of energy stress. Quantitative real-time polymerase chain reaction (qPCR) data showed a significant increase in the transcription of *ATF4*, *TXNIP*, *Sesn2*, *Trib3*, *Gdf15*, and *EIF4EBP1* in AML cells after 48 h of compound **1** treatment, suggesting significantly upregulated levels of oxidative stress (Fig. 3F). Furthermore, Western blot analysis showed a significant increase in phosphorylated AMPK after 48 h of compound **1** treatment, while total AMPK was barely affected, revealing that compound **1** induced significant energy metabolic stress (Fig. 3G). The role of excess reactive oxygen species (ROS) in triggering oxidative stress and thus promoting apoptosis in tumor therapy is compelling. Therefore, we examined the changes in ROS content. As shown in Fig. 3H, ROS levels in AML cells were elevated after 12 h of compound **1** treatment, and ROS levels were reduced at the peak of apoptosis at 48 h of treatment. However, we found that treatment with the ROS inhibitor *N*-acetylcysteine (NAC) did not reduce compound **1**-induced apoptosis, even under the double dose, there was still no significant apoptosis reduction based on the same experimental conditions and methods (Fig. S34 in Supporting information). These results suggested that apoptosis induced by compound **1** is not directly related to ROS.

Mitochondria are the primary site of intracellular ROS production. We hypothesize that the induction of oxidative stress by compound **1** is mitochondria-related. Surprisingly, we found that compound **1** significantly elevated the mitochondrial membrane potential in AML cells at 12 h, when the direct killing effect was not yet apparent, but when ROS was already elevated. The above phenomenon suggests that the mitochondria were not disrupted during the 12 h-treatment of compound **1**, resulting in a decrease in mitochondrial membrane potential (MMP) and that the elevated ROS at this time may be caused by mitochondrial respiration impairment (Figs. 3I and J). This effect is unique and differs from most antitumor drugs that damage mitochondria to reduce the MMP. The MMP is maintained by the five mitochondrial complexes that make up the mitochondrial respiratory chain through electron or proton transfer. Notably, mitochondrial complex V is the only proton pump in the respiratory chain that reduces the MMP raised by the action of the other complexes by transporting protons into the mitochondrial matrix. Therefore, we tested whether compound **1** directly reduces the activity of mitochondrial complex V. As shown in Fig. 3K, in mitochondria isolated from mouse liver, we found that compound **1** significantly inhibited the activity of mitochondrial complex V.

In summary, a novel PPAP, monosescinol A, bearing an unprecedented carbon skeleton, was isolated from *Hypericum longistylum*. To the best of our knowledge, monosescinol A is the first natural example of sesquiterpene-PPAP adduct that represented a new subclass of PPAP derivatives. Notably, monosescinol A has prominent activity against AML by directly inhibiting mitochondrial complex V, which promotes oxidative stress, endogenous inflammation, protein synthesis inhibition and even apoptosis in AML cells (Fig. 3L). The discovery of monosescinol A not only expanded the backbone of PPAP, but also paved the way for the development of PPAPs as an anti-AML drug.

Declaration of competing interest

The authors declare that they have no known competing financial interests or personal relationships that could have appeared to influence the work reported in this paper.

Acknowledgments

This work was supported financially by the National Natural Science Foundation for Distinguished Young Scholars (No. 81725021); the National Natural Science Foundation of China (Nos. 82003633 and 82104043); the National Natural Science Foundation of Hubei Province (No. 2023AFB791).

Supplementary materials

Supplementary material associated with this article can be found, in the online version, at doi:10.1016/j.cclet.2023.109458.

References

[1] F. Baron1, M. Labopin, J. Tischer, et al., J. Hematol. Oncol. 16 (2023) 10.
[2] H. Jin, Y. Zhang, S.J. Yu, et al., J. Hematol. Oncol. 16 (2023) 42.
[3] X.W. Yang, R.B. Grossman, G. Xu, Chem. Rev. 118 (2018) 3508–3558.
[4] Y. Guo, F. Huang, W.G. Sun, et al., Chem. Sci. 12 (2021) 11438–11446.
[5] S. Abe, N. Tanaka, J. Kobayashi, J. Nat. Prod. 75 (2012) 484–488.
[6] C.X. Qi, J. Bao, J.P. Wang, et al., Chem. Sci. 7 (2016) 6563–6572.
[7] S. Lin, J. Huang, H. Zeng, et al., Chin. Chem. Lett. 33 (2022) 4587–4594.
[8] F. Li, W. Sun, S. Zhang, et al., Chin. Chem. Lett. 31 (2020) 197–201.
[9] Y. Ye, N. Jiang, X. Yang, et al., Chin. Chem. Lett. 31 (2020) 2433–2436.
[10] W. Lu, Y. Zhang, Y. Li, et al., Chin. Chem. Lett. 33 (2022) 4121–4125.
[11] Z.Y. Shi, H. Hu, Y. Guo, et al., Org. Biomol. Chem. 20 (2022) 1284–1291.
[12] N. Zhang, Z.Y. Shi, Y. Guo, et al., Org. Chem. Front. 6 (2019) 1491–1502.
[13] N. Zhang, Z.Y. Shi, Q.Q. Xu, et al., Org. Lett. 22 (2020) 7926–7929.
[14] W.J. Xu, J. Luo, R.J. Li, et al., Org. Chem. Front. 4 (2017) 313–317.